iScience

CellPress
OPEN ACCESS

Article

Trimeric receptor-binding domain of SARS-CoV-2 acts as a potent inhibitor of ACE2 receptor-mediated viral entry

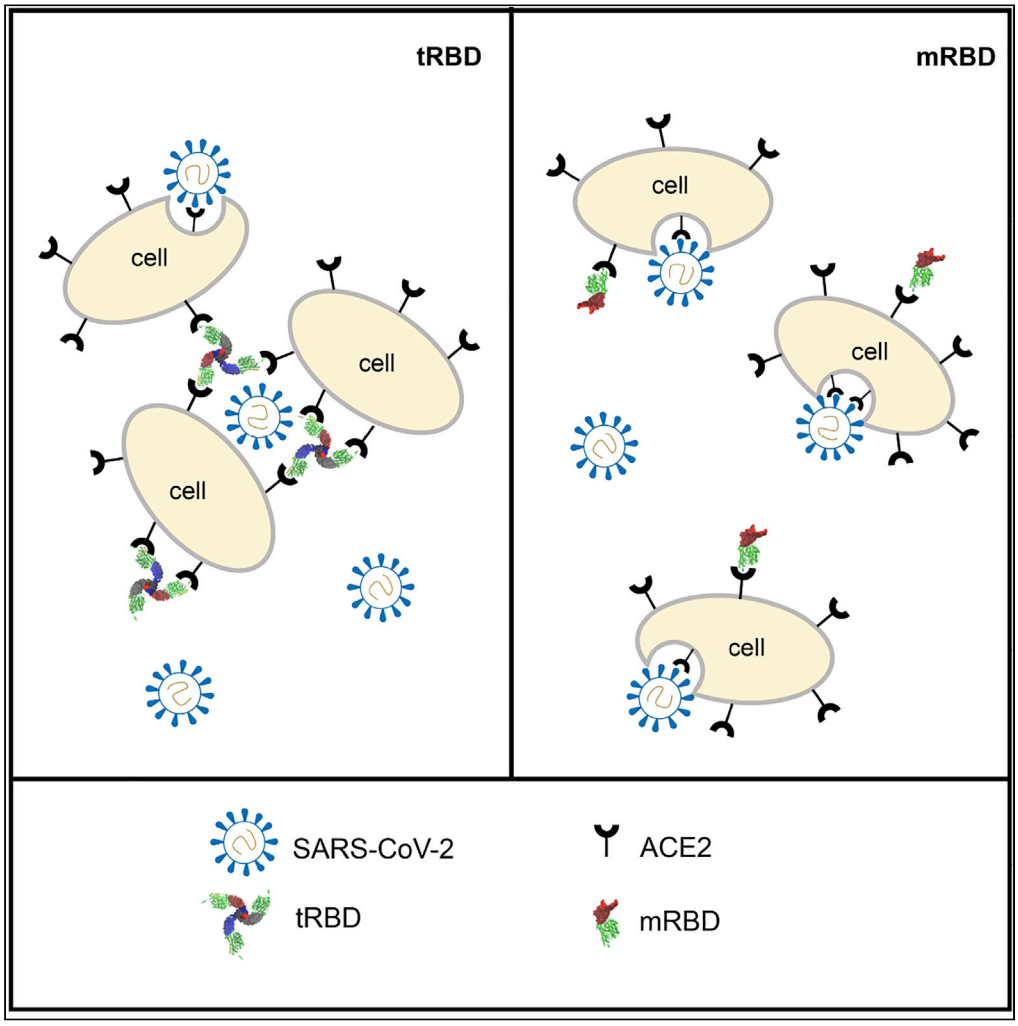

Shrikanth C. Basavarajappa, Angela Rose Liu, Anna Bruchez, ..., Tsan Sam Xiao, Matthias Buck, Parameswaran Ramakrishnan

pxr150@case.edu

Highlights

tRBD binds multiple ACE2 receptors, while mRBD and spike bind one ACE2 receptor

tRBD shows 4-fold higher inhibition of CoV-2 pseudovirus infection than mRBD

tRBD, yet not mRBD, prevents CoV-2 USA-WA1/2020 from infecting Vero cells

Use of tRBD is a potential therapeutic method to block CoV-2 infection

Basavarajappa et al., iScience *25*, 104716
August 19, 2022 © 2022
https://doi.org/10.1016/j.isci.2022.104716

iScience

CellPress
OPEN ACCESS

Article

Trimeric receptor-binding domain of SARS-CoV-2 acts as a potent inhibitor of ACE2 receptor-mediated viral entry

Shrikanth C. Basavarajappa,[1,7] Angela Rose Liu,[1,7] Anna Bruchez,[1] Zhenlu Li,[2] Vinicius G. Suzart,[1] Zhonghua Liu,[1] Yinghua Chen,[2] Tsan Sam Xiao,[1] Matthias Buck,[2,3,4,5] and Parameswaran Ramakrishnan[1,3,6,8,*]

SUMMARY

The COVID-19 pandemic has caused over four million deaths and effective methods to control CoV-2 infection, in addition to vaccines, are needed. The CoV-2 binds to the ACE2 on human cells through the receptor-binding domain (RBD) of the trimeric spike protein. Our modeling studies show that a modified trimeric RBD (tRBD) can interact with three ACE2 receptors, unlike the native spike protein, which binds to only one ACE2. We found that tRBD binds to the ACE2 with 58-fold higher affinity than monomeric RBD (mRBD) and blocks spike-dependent pseudoviral infection over 4-fold more effectively compared to the mRBD. Although mRBD failed to block CoV-2 USA-WA1/2020 infection, tRBD efficiently blocked the true virus infection in plaque assays. We show that tRBD is a potent inhibitor of CoV-2 through both competitive binding to the ACE2 and steric hindrance, and has the potential to emerge as a first-line therapeutic method to control COVID-19.

INTRODUCTION

Severe acute respiratory syndrome coronavirus type 2 (SARS-CoV-2) is the etiological cause of the ongoing 2019 coronavirus disease (COVID-19) and global pandemic (Zhu et al., 2020). The continued development of novel methods to combat SARS-CoV-2 virus entry is a top priority of current research for more efficacious disease management. As more virulent strains of SARS-CoV-2 are being discovered, successful intervention strategies to curb their cell entry are needed.

SARS-CoV-2 belongs to the betacoronavirus family and is closely related to SARS-CoV and MERS-CoV, the etiological agents of the SARS and MERS pandemics. Like other coronaviruses, SARS-CoV-2 uses a glycosylated homotrimeric class 1 fusion spike (S) protein to gain entrance into host cells. The spike protein is produced as a homotrimer in its metastable prefusion state (Kirchdoerfer et al., 2016; Walls et al., 2016). Each spike protein monomer is composed of a receptor-binding S1 domain and viral fusion S2 domain. The S1 segment specifically binds to the host cell ACE2 receptor using its highly conserved receptor-binding domain (RBD) (Wrapp et al., 2020). The main functional motif within the RBD is called the receptor-binding motif (RBM) which directly forms the interface between the spike protein and host cell ACE2 receptor (Wrapp et al., 2020). SARS-CoV-2 RBD binds to ACE2 with increased binding affinity compared to SARS-CoV owing to its more compact binding ridge and key residue substitutions. The SARS-Cov-2 spike protein, in contrast to its predecessor, also has a unique furin cleavage site between S1 and S2 (Shang et al., 2020; Walls et al., 2020; Wrapp et al., 2020). Binding of RBD and ACE2 mechanically induces the dissociation of the S1 from S2 and also allows S2 to transition into a post-binding state essential for membrane fusion. Infection of SARS-CoV-2 into several cell types has proven to require endogenous or supplemental ACE2 receptor, and SARS-CoV-2 is unable to infect cells without ACE2 receptor expression (Blanco-Melo et al., 2020; Hoffmann et al., 2020; Zhou et al., 2020). Surface colocalization of GFP-tagged ACE2 and spike protein has been observed (Wang et al., 2020), with specific binding between surface ACE2 receptor and RBD of spike protein (Lan et al., 2020). These findings support *in silico* studies which found spike protein to bind with high affinity to human ACE2 receptor (Ortega et al., 2020). Altogether the ACE2 receptor is essential for membrane fusion and viral entry.

The spike protein is organized as a trimer, with some intertwining of the subdomains. Within the spike protein, the RBD is found in the open (up) or closed (down) configurational states. Only the "up" conformation

[1]Department of Pathology, School of Medicine, Case Western Reserve University, Wolstein Research Building, 2103 Cornell Road, Cleveland, OH 44106, USA

[2]Department of Physiology and Biophysics, School of Medicine, Case Western Reserve University, Robbins Building, 2210 Circle Dr, Cleveland, OH 44106, USA

[3]The Case Comprehensive Cancer Center, School of Medicine, Case Western Reserve University, Wolstein Research Building, 2103 Cornell Road, Cleveland, OH 44106, USA

[4]Department of Neuroscience, School of Medicine, Case Western Reserve University, Robbins Building, 2210 Circle Dr, Cleveland, Ohio 44106, USA

[5]Department of Pharmacology, School of Medicine, Case Western Reserve University, Wood Building, 2109 Adelbert Road, Cleveland, Ohio 44106, USA

[6]Department of Biochemistry, School of Medicine, Case Western Reserve University, Wood Building, 2109 Adelbert Road, Cleveland, OH 44106, USA

[7]These authors contributed equally

[8]Lead contact

*Correspondence: pxr150@case.edu

https://doi.org/10.1016/j.isci.2022.104716

is able to bind ACE2 while the "down" conformation occurs when part of the binding interface is occluded from possible binding interactions (Walls et al., 2020). Structural as well as biophysical studies have revealed the nature of the up and down equilibrium (Herrera et al., 2021; Shang et al., 2020; Walls et al., 2020; Wrapp et al., 2020). It is likely that the binding of up to three ACE2 receptors to one spike trimer helps with the dissociation of the S2 and S1 segments (Benton et al., 2020). Given that the RBD:ACE2 interaction appears necessary for viral infection, the RBD of the spike protein has been a major target of interest for its potential ability to block SARS-CoV-2 viral entry. Purified RBD fragments bind strongly to human ACE2 and can block the entry of SARS-CoV-2 and SARS-CoV into human ACE2 expressing cells (Tai et al., 2020; Tian et al., 2020). A recombinant vaccine of RBD has been shown to induce functional antibody response that can neutralize SARS-CoV-2 *in vitro* and *in vivo* (Yang et al., 2020) while a recombinant RBD protein fused with human IgG1 Fc fragment was also able to induce highly potent neutralizing antibodies against SARS-CoV (He et al., 2004). Vaccines comprised of only the RBD of SARS-CoV spike protein have also shown promise previously (Chen et al., 2017; Jiang et al., 2012). Synthetic nanobodies directed against RBD have also been able to compete with ACE2 binding to neutralize SARS-CoV-2 spike pseudovirus (Custódio et al., 2020). Usage of a trimerized RBD and spike protein, as opposed to just a monomer, is expected to more closely mimic the intact live virus. Current FDA-approved vaccines consist of mRNA encoding SARS-CoV-2 full-length spike modified to remain in its homotrimeric prefusion conformation (Jackson et al., 2020; Walsh et al., 2020). However, trimerized vaccine approaches against CoV-2 are in the active developmental stage (Clover Biopharm has initiated the development of recombinant subunit-trimer vaccine based on Wuhan coronavirus (2019-nCoV), 2020). Conversely, an engineered trimeric ACE2 has been shown to bind three RBD proteins and inhibit SARS-CoV-2 infection (Guo et al., 2020; Xiao et al., 2021). An engineered RBD multimer construct coupled with an immunogenic carrier protein also induced superior immunogenicity as a multimer, than as a monomer, further suggesting the benefits of utilizing RBD multimers in SARS-CoV-2 research (Berguer et al., 2021). Tagged recombinant SARS-COV-2 RBD protein is commonly used as a tool in SARS-CoV-2 research. However, commercially available and commonly used recombinant RBD is monomeric and comprehensive studies using trimeric RBD in comparison with monomeric RBD are limited.

Here, we engineered a trimeric RBD, which is expected to mimic the tertiary structure of the SARS-CoV-2 spike protein ACE2-binding interface in physiological conditions. We hypothesized that the increased similarities of trimeric RBD to physiological conditions would competitively and potently bind to host cell ACE2, thus inhibiting viral entry at a greater efficiency than recombinant RBD monomers. We designed a mammalian expression vector to express secreted trimeric RBD by cloning RBD as a fusion protein with a leucine zipper and a leader sequence (Ramakrishnan et al., 2004). We demonstrate that our engineered RBD specifically and potently binds to the ACE2 receptor. We show that our trimeric RBD more efficiently blocks SARS-CoV-2 pseudovirus entry into ACE2 expressing cells compared to monomeric RBD *in vitro* and also blocks the entry of SARS-CoV-2 true virus and plaque formation in Vero cells. The study demonstrates a head-to-head comparison of trimeric and monomeric RBD and shows that the use of engineered trimeric RBD is a superior method to the use of monomeric RBD, to inhibit SARS-CoV-2 infection in cellular systems.

RESULTS

Trimeric receptor-binding domain expression in HEK 293T cells

Given the importance of the trimeric nature of the native spike protein to potently bind to host cells, we hypothesized that an engineered trimeric RBD (tRBD) would have the ability to similarly bind to multiple ACE2 receptors on host cells, and outcompete the SARS-CoV-2 virus for cell entry. We cloned the RBD region into a mammalian expression vector in fusion with a modified leucine zipper to induce trimerization, a leader sequence to allow the secretion of the recombinant protein, and FLAG or HIS epitope tag to allow purification (Figure 1A).

We transfected HEK293T cells with our engineered tRBD plasmid to produce FLAG or HIS-tagged tRBD or HIS-tagged mRBD. The culture supernatants were assessed at the time points indicated by Western blotting. The highest expression of FLAG-tRBD (Figure 1B top) and HIS-tRBD (Figure 1B bottom) was observed at 72 h post-transfection. Thus, 72 h post-transfection period was chosen for collecting the conditioned media containing tRBD or mRBD for purification and use in all further experiments as described in the flow chart (Figure 1C). We estimated the amounts of tRBD and mRBD in the conditioned media 72 h post-transfection by Western blotting and densitometry analysis (Figure 1D). A linear regression equation was obtained by plotting the densitometry values of increasing concentrations of commercially

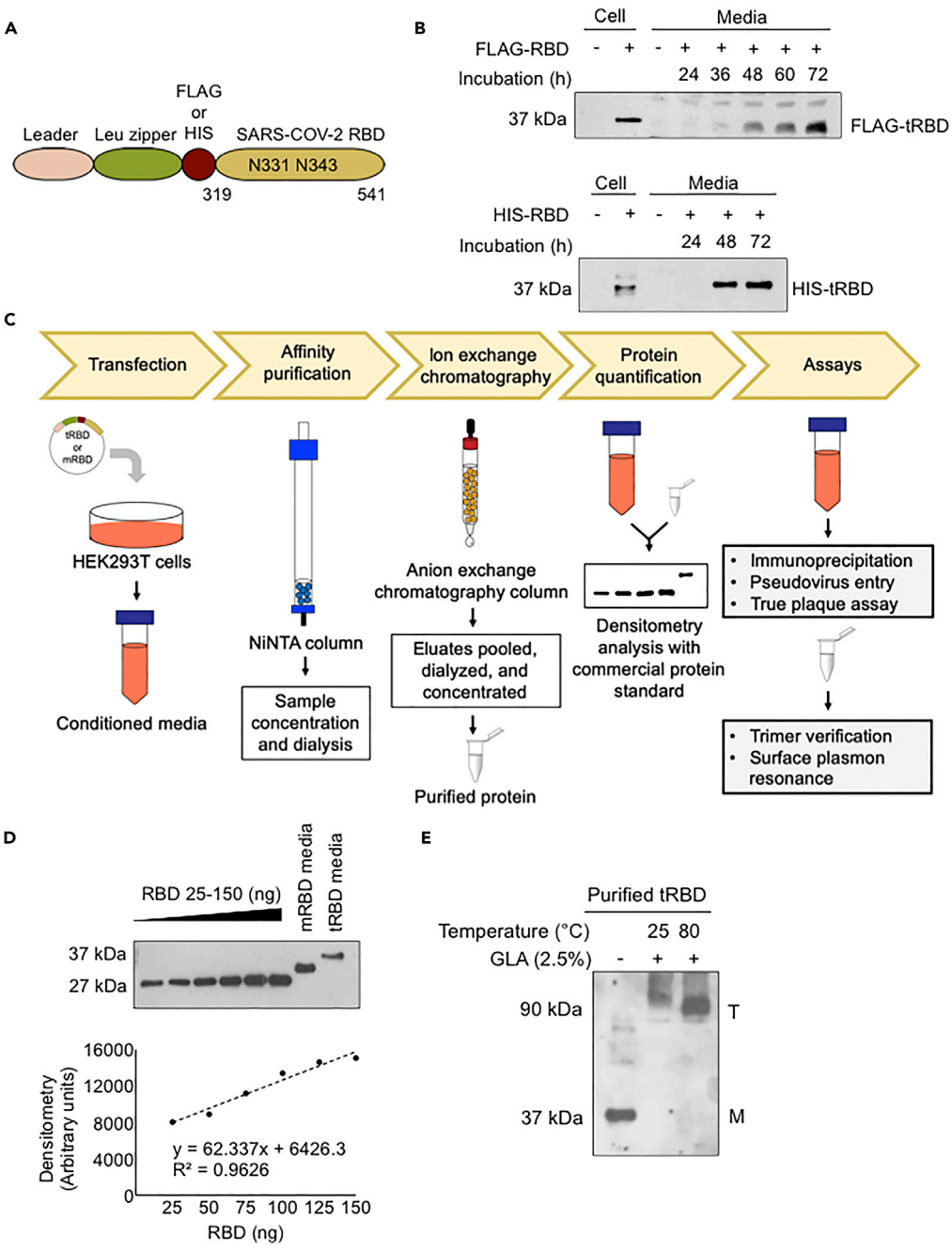

Figure 1. Construction and expression of tRBD and mRBD *in vitro*

(A and B) (A) Liner representation of FLAG or HIS-tagged SARS-COV-2 RBD construct sequence for the expression of tRBD (B) Expression levels of FLAG-tagged (top) or HIS-tagged (bottom) tRBD at varying timepoints after transfection of HEK293T-ACE2 cells.

(C) Schematic representing protocol for tRBD and mRBD protein purification.

(D) Varying concentrations of HIS-tagged commercially available recombinant SARS-COV-2 RBD protein (Lane 1–6), and conditioned media with HIS-tagged mRBD (Lane 7) or HIS-tagged tRBD (Lane 8) was separated via SDS/PAGE gel and probed with anti-HIS antibody. A linear regression curve was constructed using densitometry analysis.

(E) tRBD was crosslinked with glutaraldehyde (GLA) and incubated at temperatures indicated. Crosslinked proteins were separated in SDS/PAGE gel and probed with anti-HIS antibody. (n = 2 independent samples).

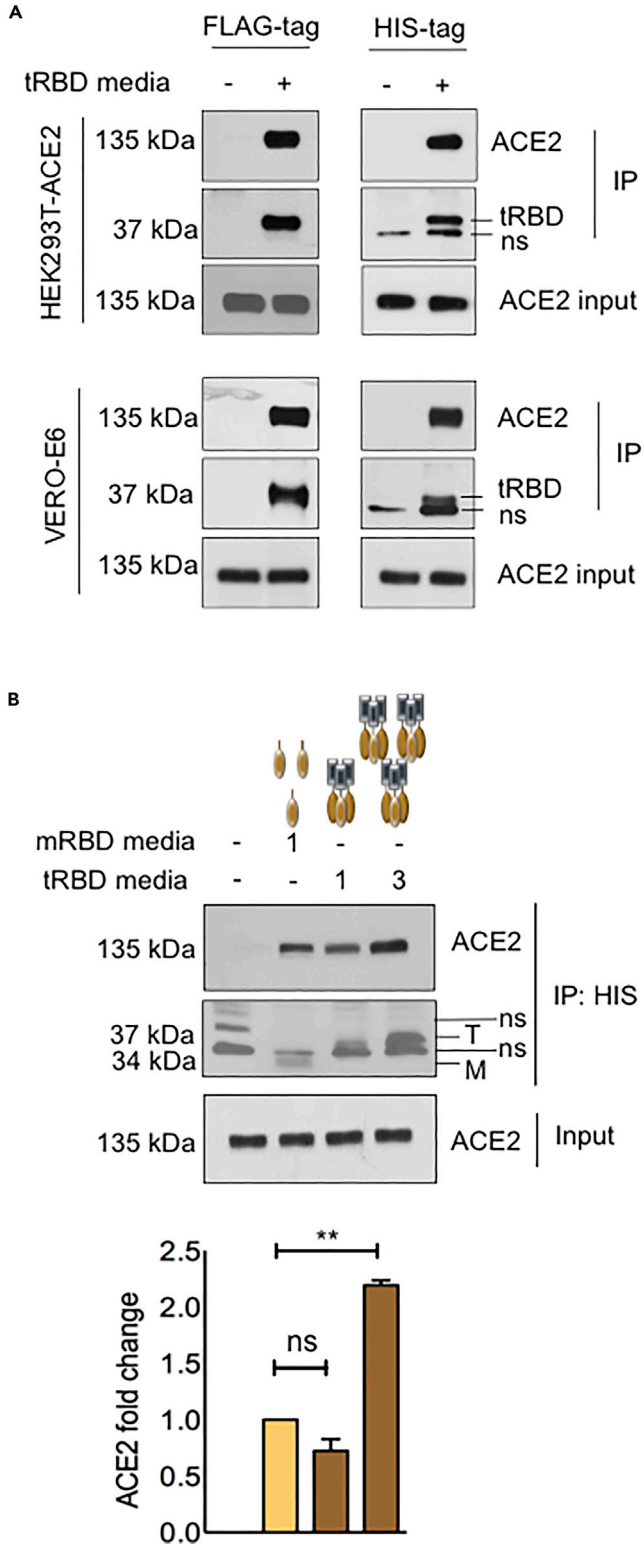

Figure 2. *In vitro* binding ability of RBD:ACE2

(A and B) HEK293T-ACE2 cells (3×10^5) or Vero E6 cells (8×10^5) were plated 24 h prior in 6 and 10 cm plates, respectively. (A) HEK293T-ACE2 cells were treated with 2.5 mL of FLAG-tagged tRBD (left) or HIS-tagged tRBD (right). Vero E6 cells were treated with 5 mL of FLAG-tagged tRBD or HIS-tagged tRBD (bottom). (B) HEK293T-ACE2 cells were treated with

Figure 2. *Continued*
666.7 ng/mL of HIS-tagged mRBD (indicated as one in the figure) or tRBD (indicated as one in the figure) or 2000 ng/mL of HIS-tagged tRBD (indicated as three in the figure). Thirty minutes following incubation, cells were assessed by immunoprecipitation using (A, left) anti-FLAG or (A, right and B) NiNTA Agarose beads. (B, bottom) Densitometry analysis of three independent Western blots as in Figure 2B, top, presented as mean ± SE of mean (SEM). **p< 0.01, ns - non significant.

available recombinant RBD in the range of 25–150 ng. This calibration plot was used to quantitate the amount of mRBD and tRBD in the subsequent experiments. tRBD and mRBD were purified from conditioned media using NiNTA Agarose affinity purification and ion-exchange chromatography (Figure 1C). We obtained approximately 819 μg of mRBD and 115 μg of tRBD per liter of transfected HEK293T cell culture supernatant. To confirm the trimeric nature of tRBD, purified tRBD was crosslinked with glutaraldehyde and incubated at 25°C or 80°C. Analysis by Western blot confirmed the trimeric nature of tRBD at ~90 kDa (Figure 1E). We also found a temperature-dependent increase in cross-linking efficiency observed at 80°C compared to 25°C.

Receptor-binding domain trimer interacts more efficiently with ACE2 than receptor-binding domain monomer

To obtain direct evidence that our engineered tRBD interacts with ACE2 receptor on host cells, we treated HEK293T cells stably expressing the ACE2 receptor (HEK293T-ACE2) with FLAG-tagged or HIS-tagged tRBD and performed immunoprecipitation using anti-FLAG antibody (Figure 2A, left) or NiNTA beads (Figure 2A, right), respectively (Figure 2A, left). The assessment of immunoprecipitates confirmed that tRBD is able to bind to ACE2 *in vitro*. To exclude the possibility that the binding of tRBD to ACE2 is owing to the overexpression of ACE2 in HEK293T cells, we used Vero cells, which express endogenous ACE2 receptor and demonstrated that similar to HEK293T-ACE2 cells, tRBD binds to endogenously expressed ACE2 receptor (Figure 2A, bottom).

Because tRBD contains three RBD units, we hypothesized that tRBD would bind more ACE2 than mRBD. To compare the binding abilities of tRBD and mRBD to ACE2, we incubated conditioned media containing HIS-tagged tRBD or mRBD with HEK293T-ACE2 cells. We estimated the total RBD protein concentration in the conditioned media expressing tRBD and mRBD using the commercial recombinant HIS-RBD protein as a standard (Figure 1D), and examined two different amounts of tRBD to study ACE2 binding. First, we treated cells with normalized total protein concentration of RBD in the conditioned media. This yielded one-third of the tRBD structural units compared to mRBD (Figure 2B, mRBD one and tRBD 1, lanes two and 3), as a single tRBD is comprised of three RBD units while a single mRBD only has one RBD unit. When used at equal protein concentrations, we found that mRBD and tRBD were able to bind similar amounts of ACE2. Next, we used three times the concentration of tRBD to normalize the number of mRBD and tRBD structural units (Figure 2B, mRBD one and tRBD 3, lanes two and 4). When equal amounts of structural units of tRBD and mRBD were used, tRBD was able to bind to and precipitate significantly higher amounts of ACE2. Taken together, this suggests that one-third structural units of tRBD are sufficient to bind and precipitate the same amounts of ACE2 as mRBD, directly showing that tRBD and ACE2 are able to bind potently (Figure 2B).

Molecular modeling of the binding of receptor-binding domain monomer and trimer to the ACE2 receptor

Our *in vitro* data determined that tRBD is able to bind to ACE2 receptor more potently than mRBD. We performed molecular modeling to confirm these results and comparatively studied the binding of mRBD and tRBD to the ACE2 receptor in silico (Figures 3A–3D). Our modeling studies suggest that similar to the native spike protein, mRBD can only bind to ACE2 receptor through a single RBD receptor-binding motif (RBM) (Figure 3C). However, our engineered tRBD can interact with up to three ACE2 receptors using all three RBM (Figure 3D), potentially forming larger scale networks (see discussion). Because the linker between the coiled-coil region (the leucine zipper) and the RBD is flexible and of sufficient length, the RBD may change orientation. However, even a single trimer may bind ACE2 more strongly by turning two of the RBDs by 180° allow both domains to bind to an ACE2 dimer simultaneously (Figure 3D), with the third RBD engaging a separate ACE2.

We next studied the real-time interaction between ACE2 and tRBD or mRBD using surface plasmon resonance (SPR). Biotinylated ACE2 was captured on a streptavidin sensor chip and binding assays were performed with different concentrations of purified mRBD or tRBD. Representative sensorgrams for

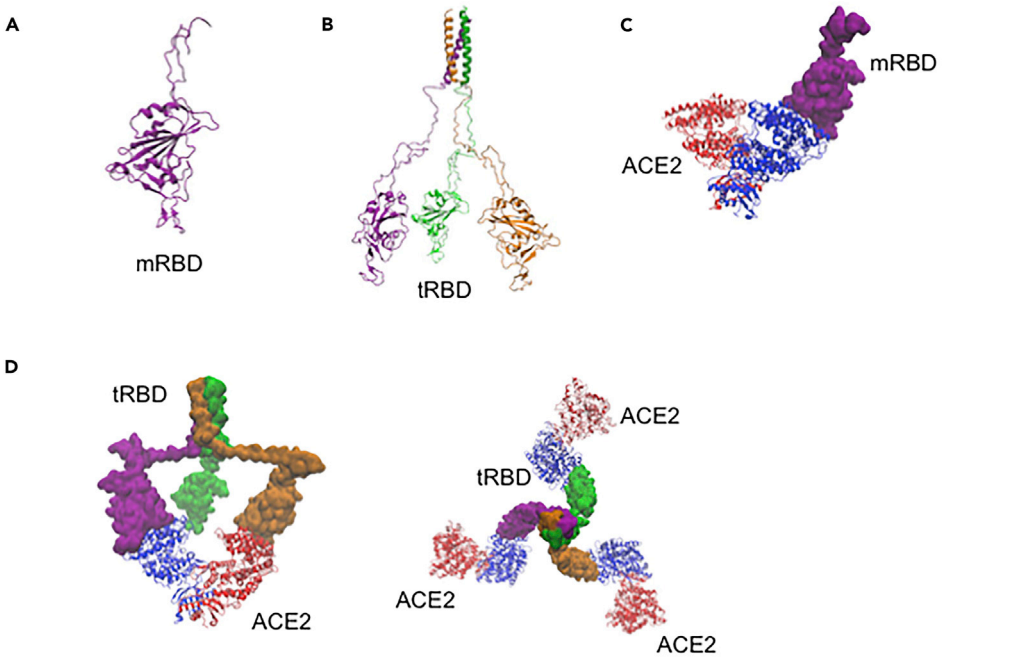

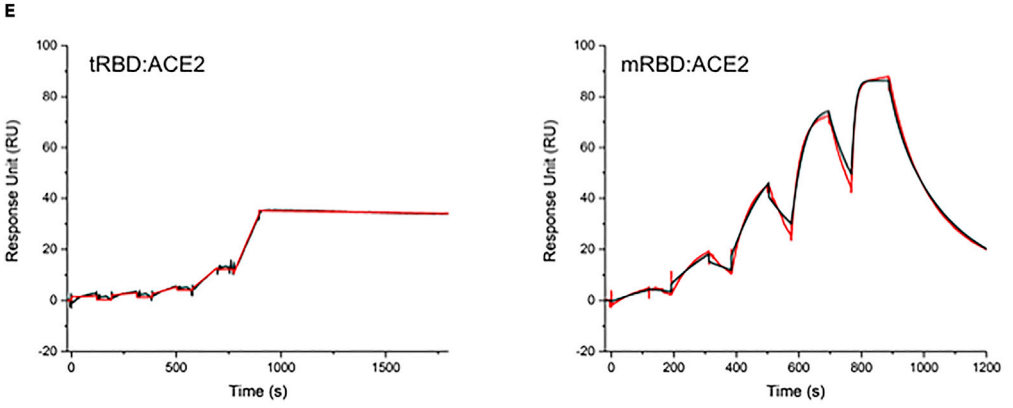

F

Analyte	Ligand	ka(1/Ms)	kd (1/s)	K_D (nM)
mRBD	ACE2	2.96E+05	7.26E-03	30 ± 15.14
tRBD	ACE2	9.95E+04	3.54E-05	0.51 ± 0.33

Figure 3. Molecular modeling and surface plasmon resonance data

(A–D) Structure of (A) monomeric RBD (mRBD) and configuration of (B) trimeric RBD (tRBD). (C) Binding models of mRBD with ACE2 dimer; (D) Binding models of tRBD with ACE2. tRBD binds to two units of an ACE dimer (left) as RBDs can rotate relative to one another, or binds to three separate ACE2 dimers (right).

(E) Representative binding sensorgrams for mRBD:ACE2 and tRBD:ACE2 interactions using the single cycle kinetic assay. Binding sensorgrams were generated from five independent injections of mRBD/tRBD. Black and red lines represent fitted curves generated by 1:1 binding.

(F) mRBD or tRBD in running buffer (PBSP+, pH7.4 purchased from Cytiva) were flowed over three surfaces with a density of 500–1500RU biotin-ACE2 on an S series SA sensorchip in a Biacore T200 system. Mean kinetic rate constant K_a, K_d and the equilibrium dissociation constant ($K_D = K_d/K_a$) were measured from single-cycle kinetics and globally fitted by BiaEvaluation 3.1 software using 1:1 binding model, three sets of data were averaged and standard errors for the affinity values are shown.

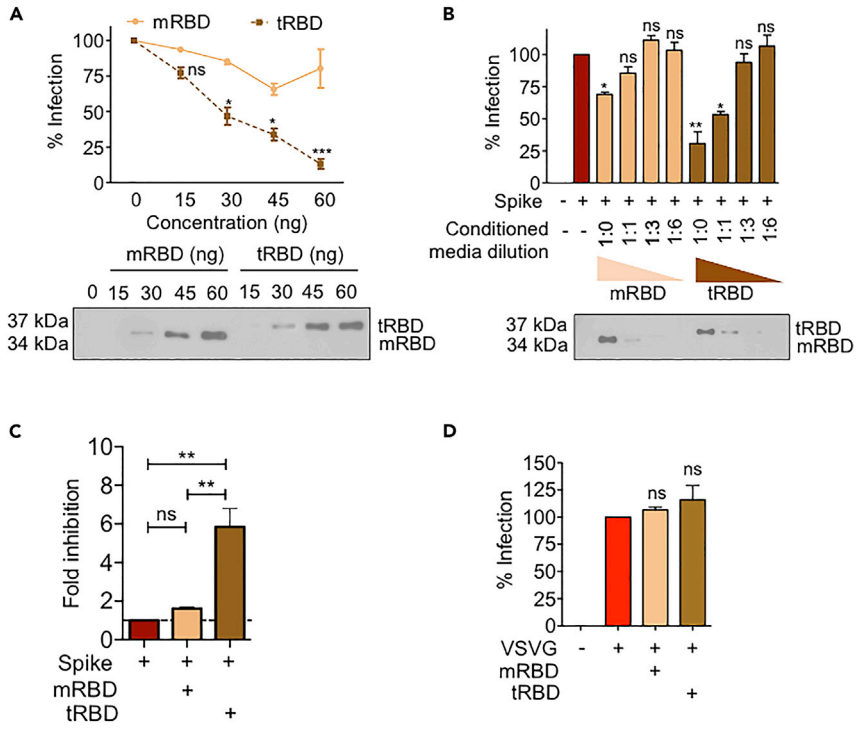

Figure 4. tRBD-mediated inhibition of SARS-COV-2 pseudovirus cell entry in HEK293T-ACE2 cells

(A–D) HEK293T-ACE2 cells (1.25×10^4 cells/well) were treated with specified amounts of HIS-tagged mRBD or HIS-tagged tRBD. (A and B) SDS/PAGE gel was used to verify equal concentrations of mRBD or tRBD was used. (A–C) SARS-CoV-2 pseudovirus (1:0) or (D) VSVG virus (1:50) with the Luciferase-IRES-ZsGreen backbone were produced via calcium phosphate transfection and co-treated onto HEK293T-ACE2 cells. Luciferase activity was assessed and values are presented as RLU of infected cells treated with tRBD or mRBD over cells infected with pseudovirus alone. Data are representative of three independent experiments conducted in triplicates and are presented as mean ± SE of mean (SEM). Statistical significance was analyzed using two-tailed Student's unpaired t test, *p < 0.05; **p < 0.01, ***p<0.001, ns – non significant.

tRBD (Figure 3E, left) and mRBD (Figure 3E, right) are shown. To calculate kinetic parameters, a 1:1 Langmuir data fitting was applied to the sensorgrams. Our engineered tRBD showed a dissociation rate of 3.54×10^{-5} 1/s while mRBD showed a much faster dissociation rate of 7.26×10^{-3} 1/s (Figure 3F). This indicates that tRBD has a higher affinity to ACE2 than mRBD. The binding affinity K_D between mRBD and ACE2 was detected to be 30 nM, which is consistent with the binding affinity reported in previous studies (Kim et al., 2021; Lan et al., 2020; Liu et al., 2021). Importantly, our engineered tRBD binds ACE2 with a 58.8-fold higher affinity (K_D = 0.51 nM) than mRBD (K_D = 30 nM), further supporting our molecular modeling data indicating that tRBD binds to ACE2 with higher affinity than mRBD.

Receptor-binding domain trimer block SARS-COV-2 pseudovirus entry into ACE2 expressing cells

Our biochemical binding studies suggested that tRBD binds to ACE2 very potently and our molecular modeling indicated the plausible spatial orientation of the tRBD binding to ACE2. We then hypothesized that tRBD's structure would prove advantageous to outcompete native spike protein and occupy host cell ACE2 to prevent viral entry. To test the functional effect of tRBD:ACE2 binding, we utilized a luciferase reporter system to measure the amount of pseudoviral entry into HEK293T-ACE2 cells as previously described (Crawford et al., 2020). Cells were incubated with equal concentrations of tRBD or mRBD simultaneously with pseudovirus for 48 h. Infectivity of SARS-CoV-2 was assessed by viral-entry-dependent luciferase expression (RLU). Starting at 30 ng, tRBD was able to better inhibit pseudovirus entry into HEK293T-ACE2 cells than mRBD (Figure 4A). Next, we assessed the separate abilities of various dilutions of mRBD and tRBD to inhibit pseudoviral entry. Although mRBD only showed moderate pseudoviral entry inhibition at 50 ng, tRBD showed significant pseudoviral entry inhibition at both 50 and 25 ng dilutions

(Figure 4B). At the highest concentration tested, mRBD showed only 1.6-fold inhibition, while tRBD showed about 6-fold inhibition of pseudoviral entry (Figure 4C). Thus, tRBD was found to be able to inhibit pseudovirus entry about 4 times better than mRBD. This demonstrates the functional advantage of our trimeric tool in its ability to occupy ACE2 receptors and inhibit the spike-mediated viral infection of host cells. To ensure that mRBD and tRBD inhibition was specific to spike:ACE2-mediated viral entry, we treated infected HEK293T-ACE2 cells with a VSV-G pseudotyped virus, without or with mRBD or tRBD. VSV-G has a broad cell tropism which enables it to infect most mammalian cell types (Gillies and Stollar, 1980; Seganti et al., 1986). We found that both tRBD and mRBD were unable to block the VSV-G-mediated viral infection of HEK293T-ACE2 cells (Figure 4D), showing that mRBD and tRBD selectively blocks spike-ACE2-mediated viral entry.

Trimeric receptor-binding domain blocks SARS-CoV-2 infection

To validate the inhibition findings from infection with the pseudovirus, we confirmed the ability of tRBD to block infectious SARS-CoV-2 by using an isolate of the true virus (USA-WA1/2020) for *in vitro* infection of Vero E6 cells. Vero E6 cells are completely susceptible to SARS-CoV-2 without exogenous overexpression of ACE2 and are commonly used for SARS-CoV-2 propagation and plaque assays. We first pre-incubated these cells with varying concentrations of mRBD and tRBD for 30 min prior to infection. We then assessed the percentage of infectivity of SARS-CoV-2 by measuring the number of plaque-forming units per milliliters (PFU/mL) 72 h post-infection. Representative images of the plaques not only show a reduction in the overall number of plaques that are formed but also a reduction in the average diameter of the plaques at high tRBD concentrations (Figure 5A). This indicates that the tRBD can prevent the entry of virus into cells and also, when present at high enough concentrations, can inhibit subsequent spread to adjacent cells after initial infection occurs. Furthermore, similarly to infection with the pseudovirus, SARS-CoV-2 infection increased at the highest media dilutions of tRBD, proving that the ability of tRBD to block SARS-CoV-2 infection is impaired at lower concentrations. In contrast, mRBD did not evoke much inhibition when compared to Mock (Mk) media in the infectious SARS-CoV-2 assays, even in the undiluted mRBD media (Figure 5B). The dose-response curve for tRBD indicated the dosage at which 50% of infectious virus was inhibited (inhibitory concentration 50 or IC50) is equal to 1602 ng/mL (95% CI 1209–2,198 ng/mL) (Figure 5C). Thus, tRBD inhibits SARS-CoV-2 infectivity in a dose-dependent manner by competing with the viral spike protein for ACE2 binding on the host cell.

DISCUSSION

While exploring the methods to block CoV-2 infection, we found that the spike RBD was commonly studied and sold in a monomeric form, while the actual spike protein is a trimer. We realized that comprehensive studies using trimeric RBD are limited and this prompted us to model and generate a trimeric RBD. We hypothesized that the trimer may block the spike-mediated viral entry better than the monomer. In addition, the use of trimeric RBD may provide double advantage in blocking the viral infection and serve as an immunogen to generate anti-CoV-2 antibodies when used as a therapeutic agent in the host organism.

In this study, we utilized the RBD region of the spike protein of SARS-CoV-2 virus to create a trimeric RBD, which effectively inhibited the entry of both psuedotyped and true SARS-CoV-2 virus. We focused on the RBD region because it is the mediator of host cell engagement and is highly conserved between various betacoronaviruses. Our focus was to develop a method to block RBD:ACE2 engagement. Recent studies have also described the ability of recombinant RBD fragment protein to block SARS-CoV-2 infection (Tai et al., 2020). The monomeric and trimeric RBD show significant differences in their three-dimensional structure (Figures 3A–3D), leading us to hypothesize that usage of either entity would result in different biological outcomes. We also suspected that trimerizing RBD protein would more mimic the actual virus conformation, and therefore lead to more favorable binding to ACE2. In our study, we show that trimeric RBD is superior to monomeric RBD in binding to ACE2 (Figures 2 and 3), blocking spike-mediated viral infection in pseudoviral assay (Figure 4) and in blocking true virus infection (Figure 5). RBD trimer was able to block viral entry about 4 times better than monomeric RBD, likely in part owing to the reorientation that is possible of the RBDs in the trimer, allowing it to bind an ACE2 dimer from both sides. The dissociation constant K_D of SARS-CoV-2 has consistently been reported to be lower than that of SARS-CoV (Nguyen et al., 2020; Walls et al., 2020; Wrapp et al., 2020), thus it is plausible that the trimeric CoV-2 RBD may also block ACE2 binding of other betacoronaviruses such as SARS-CoV and MERS-CoV. Moreover, the efficacy of tRBD can be increased upon potential SARS-CoV-2 infection because if many ACE2 receptors are close in proximity, in principle, the higher local concentration of the RBDs in a trimer is

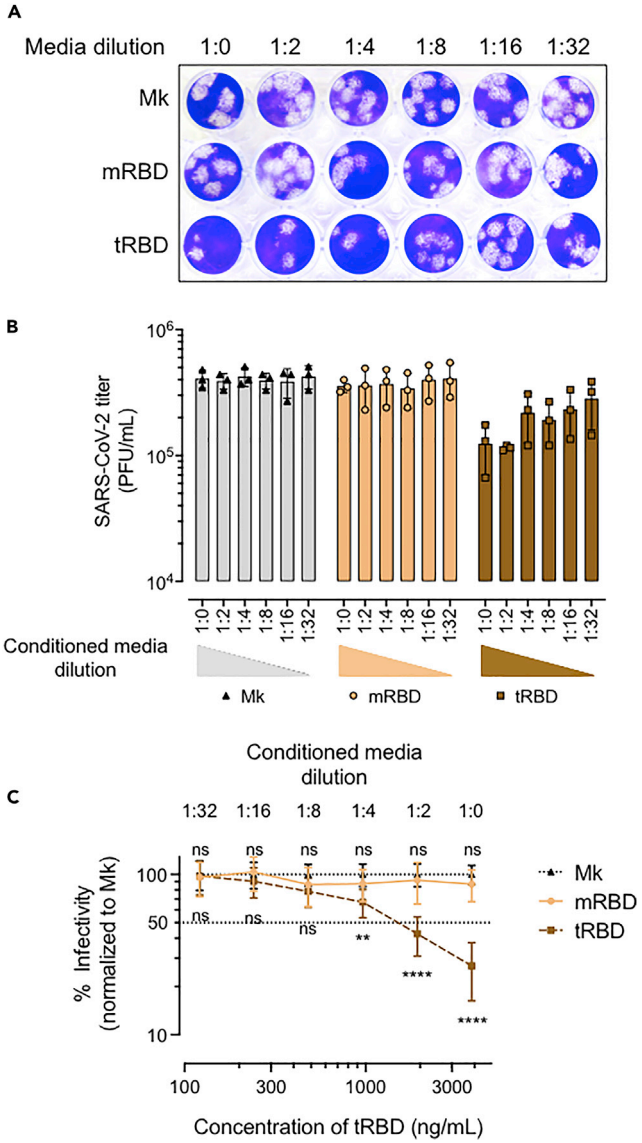

Figure 5. SARS-CoV-2 Plaque reduction assay

(A and B) Vero E6 cells grown in 24-well plates were incubated with undiluted (1:0) or 2-fold serially diluted mRBD (●), tRBD (■), or media (Mk-▲) for 30 min prior to SARS-CoV-2 infection. (A) Representative images of plaque formation on Vero E6 cells in the presence of the indicated conditioned media. (B) Plaque-forming units per milliliter (PFU/mL) were measured 72 h post-infection and values of three independent experiments, each conducted in triplicate, were combined. Individual data points represent the mean titer for each experiment. Bar plots indicate the mean of the individual experiments for each condition tested ±standard errors of mean values (SEM).

(C) Dose-response curve with normalized values from (B) graphed to represent the mean of three independent experiments, each value was normalized to the Mk titer of SARS-CoV-2 for the media dilution independently for each experiment performed. Error bars represent 95% confidence interval. (B and C) Significance was determined by ANOVA with Dunnett's multiple comparison test. *$p < 0.05$; **$p < 0.01$; ****$p < 0.0001$, presented as mean ± SE of mean (SEM).

expected to allow a faster Kon rate for the second ACE2:RBD pair, but a slower rate is seen suggesting a configurational change. The Koff for a single ACE2:RBD interaction is expected to be similar for both the mRBD and tRBD, but the positive cooperativity in different RBDs of tRBD probably slowed the dissociation rate (Figure 3). Furthermore, just as in the natural spike protein trimer, three ACE2 dimers may bind to one RBD trimer through one of the ACE2 units, leaving the second unit for binding to another RBD trimer. Thus, potentially a 2D network is formed on the surface of the cell. Thus, based on our molecular modeling and

biochemical-binding studies as well as biophysical assays, we speculate that the trimeric RBD may simultaneously bind multiple ACE2 receptors in its vicinity. It is plausible that these tRBD:ACE2 complexes are associated with one cell or the adjacent cells, ultimately resulting in a reduced availability of ACE2 sites for the real virus infection (See graphical abstract for the speculative model).

The important role that the spike protein has in membrane fusion and viral infection has made it a primary target for the development of small molecular inhibitors, antibody therapy, and vaccines. The outpouring of research after the outbreak of the coronavirus pandemic has resulted in many potential drugs targeting different portions of the SARS-CoV-2 spike protein (Huang et al., 2020). Vaccine strategies have also pinpointed different portions of the spike protein to generate host cell immunogenicity. There are several ongoing efforts toward developing trimerized full-length spike protein as well as the utilization of RBD protein to elicit an immune response for virus protection (W. H. Chen et al., 2020b). One of the RNA-based vaccine candidates evaluated by Pfizer encoded a trimerized SARS-CoV-2 RBD which was able to elicit a robust humoral and cell-mediated antiviral response (Walsh et al., 2020) showing the potential efficacy and feasibility of using tRBD as therapeutics. Previous studies following the SARS pandemic in 2003 have also shown the advantages of an RBD-based vaccine to minimize host reactivity with efficient viral neutralizing ability (Jiang et al., 2012). Recent studies have also demonstrated the ability of engineered trimeric RBD proteins to effectively elicit neutralizing antibodies in hosts (Malladi et al., 2021; Routhu et al., 2021). Our engineered trimer supports published literature (Liu et al., 2021; Xiong et al., 2020) which suggests that the flexibility and molecular similarity of a trimeric RBD protein to the native spike protein is a promising therapeutic approach to combating SARS-CoV-2. Our modeling and binding studies suggests that the engineered tRBD possesses flexibility to interact with up to three ACE2 receptors. The ability of our engineered RBD to reorient gives it the potential to form larger scale networks. This tri-prong binding likely provides an avidity effect, which is not possible in the natural spike protein trimer, as the RBDs cannot reorient. This gives an advantage for our engineered trimeric RBD to bind to and block ACE2 receptor's spike-binding regions. We used a modified leucine zipper that has isoleucine substitutions at the *a* and *d* positions to allow for trimer formation, in contrast to the dimers formed from traditional GCN4 leucine zippers (Harbury et al., 1994). The modified leucine zipper is widely used in biomedical research for therapeutics that require trimerization for their activity, including drugs that have been tested preclinically (Melchers et al., 2011; Morris et al., 2007; Rozanov et al., 2009) and clinically (Morris et al., 1999; Vonderheide et al., 2001). Interestingly, trimeric protein vaccines utilizing a modified leucine zipper against HIV (Melchers et al., 2011), respiratory syncytial virus (Rigter et al., 2013), and influenza virus (Cornelissen et al., 2010; Loeffen et al., 2011; Rigter et al., 2013) have proven successful preclinically. Despite the extensive use of this modified leucine zipper in both preclinical and clinical models, it is possible that this trimerization protein domain has immunogenic potential. However, a mutated modified leucine zipper with specific N-linked glycosylation sites has been described to successfully dampen leucine-zipper-induced immunogenicity but not affect protein multimerization or immune response to the antigens fused to the zipper (Sliepen et al., 2015). The breadth of literature to support the successful usage of a modified leucine zipper for protein trimerization in therapeutics made us confident that this was a valid and useful approach to designing a tool against the SARS-CoV-2 virus.

Our study is unique in that it demonstrates a comparative evaluation of the monomeric and trimeric RBD in binding to the ACE2 receptor and their molecular ability to block SARS-CoV-2 host cell infection through competitive inhibition. This biochemical study provides valuable mechanistic and pharmacological information that can be utilized in improving trimeric RBD-based therapeutic development. Such an evaluation may prove valuable in designing novel therapeutic methods for CoV-2 as well as other viruses that employ a similar mechanism of infection. Paired with previous publications showing the ability of trimeric RBD to elicit neutralizing antibodies, we thus believe that our study suggests that the usage of a trimeric RBD can deliver therapeutic potential using a two pronged approach: 1) protecting hosts from future infection via antibody response and 2) protection from current SARS-CoV-2 viral infection prior to antibody production. Further development of our engineered tRBD could be used as a therapeutic to stop SARS-CoV-2 infection from spreading to neighboring cells after clinical detection.

SARS-CoV-2 is continuing to evolve and mutate. Many of these mutations entail amino acid changes in the receptor-binding motif (RBM) where the RBD is in direct contact with ACE2 to improve RBD:ACE2 binding (J. Chen et al., 2020a). These mutations, while not more pathogenic, are more infectious. Specific mutation variants have become resistant to some neutralizing antibodies (Li et al., 2020). We are unsure if our engineered RBD trimer generated using the wild type protein sequence will outcompete the mutated virus;

however, this approach can be validated for any mutant variants of the virus by generating vectors with site-specific mutations in the RBD domain. Furthermore, viral mutations that improve RBD:ACE2 binding provide important insight into how to continuously improve our engineered trimer in the future. By analyzing the mutations that result in improved receptor binding, we will be able to improve our current trimer to further improve viral entry blockade.

We view our engineered trimer as a complement to the SARS-CoV-2 vaccines that have been recently approved by the FDA. Although the SARS-CoV-2 vaccines have a >90% efficacy, they require multiple doses leaving a latency period before virus protection begins (Moderna, 2020; Rose et al., 2020). As with all vaccines, there will also be a population who will fail to mount an effective amount of neutralizing antibodies, particularly in high-risk populations (Goodwin et al., 2006). In the future, molecules such as our RBD trimer can be delivered simultaneously or prior to vaccines to confer more antiviral protection. This use of combinatorial therapeutic approaches will confer improved protection from SARS-CoV-2 and also will help prevent the induction of more severe infection.

Limitations of the study

We have generated an enforced trimeric RBD using a modified leucine zipper domain. It is not clear whether such an approach will cause any unwanted effects when used *in vivo*. Although our molecular modeling, *in vitro* and in true virus studies show the efficacy of the trimeric RBD, the actual structural details of how it binds and blocks CoV-2 infection are not known. As the trimeric RBD is likely able to bind to multiple ACE2 receptors at the cell surface, it remains to be determined whether it will cause the activation of cellular signaling downstream of the ACE2 receptor.

STAR★METHODS

Detailed methods are provided in the online version of this paper and include the following:

- KEY RESOURCES TABLE
- RESOURCE AVAILABILITY
  - Lead contact
  - Materials availability
  - Data and code avilibility
- EXPERIMENTAL MODEL AND SUBJECT DETAILS
  - Cells
  - Virus
- METHOD DETAILS
  - Molecular modeling
  - Recombinant protein expression and purification
  - Quantification of secreted tRBD and mRBD in culture media
  - Chemical crosslinking of tRBD
  - Immunoprecipitation and western blotting
  - Surface plasmon resonance
  - Luciferase assay
  - SARS-CoV-2 plaque reduction assay
- QUANTIFICATION AND STATISTICAL ANALYSIS

ACKNOWLEDGMENTS

We thank Dr. Jesse Bloom and Katharine Crawford (Fred Hutchinson Cancer Research Center; Seattle, WA) for the providing the SARS-CoV-2 spike pseudotyped lentiviral expression system. We thank Dr. Florian Krammer (Icahn School of Medicine at Mount Sinai, New York) for providing the mammalian vector expressing secreted monomeric HIS tagged RBD (pCAGGS-HIS RBD) and Maria Iannucci (Case Western Reserve University, Ohio) for support with biophysical assays. Funding. A pilot funding to P.R. from Eric and Jane NORD Family Fund for COVID related research primarily supported this study. P.R. is supported by NIH/NIAID grants R01AI116730 and R21AI144264, NIH/NCI grant R21 CA246194. M.B. is currently funded by NIH R01 grant from the National Eye Institute R01EY029169 and his part of the project was also supported by pilot grant from the Department of Physiology and Biophysics of Case Western Reserve University. T.S.X. is supported by NIH grants R01GM127609 and P01AI141350. A.R.L. is supported by the National Institutes of Health NIH/NEI T32 pre-doctoral training grant T32EY007157. SARS-CoV-2 work was performed

in the BSL3 at Case Western Reserve University (CWRU), which is supported by the CWRU and University Hospitals Center for AIDS research grant P30AI36219.

AUTHOR CONTRIBUTIONS

Conceptualization, P.R. Methodology, P.R, A.B, M.B, T.S.X., Investigation, S.B., A.R.L, A.B., Z.Li, V.S., Z.L, Y.C, P.R. Writing – Original Draft, S.B., A.R.L., A.B., M.B., P.R. Writing – Review & Editing, S.B, A.R.L, A.B., Z.Li, V.S., Z.L., T.S.X., M.B., P.R. Visualization, S.B., A.R.L, A.B., Z.Li, PR. Supervision, P.R., A.B., M.B., T.S.X. Project Administration, P.R. Funding Acquisition, P.R, A.B., M.B., T.S.X.

DECLARATION OF INTERESTS

PR has submitted an invention disclosure 2020–3814, on the use of trimeric RBD as a multipotential therapeutic target to Case Western Reserve University. All other authors declare no conflict of interest in this study.

Received: August 4, 2021
Revised: May 12, 2022
Accepted: June 29, 2022
Published: August 19, 2022

REFERENCES

Benton, D.J., Wrobel, A.G., Xu, P., Roustan, C., Martin, S.R., Rosenthal, P.B., Skehel, J.J., and Gamblin, S.J. (2020). Receptor binding and priming of the spike protein of SARS-CoV-2 for membrane fusion. Nature *588*, 327–330. https://doi.org/10.1038/s41586-020-2772-0.

Berguer, P.M., Blaustein, M., Bredeston, L., Craig, P.O., D'Alessio, C., Elias, F., Farré, P.C., Fernández, N.B., Gentili, H.G., Gándola, Y., and Gasulla, J., Gudesblat, G.E., Herrera, M.G., Ibañez, L.I., Idrovo-Hidalgo, T., Nadra, A.D., Noseda, D.G., Paván, C.H., Pavan, M.F., Pignataro, M.F., Roman, E., Ruberto, L.A.M., Rubinstein, N., Sanchez, M. V, Santos, J., Wetzler, D.E., Zelada, A.M.. (2021). Production of a highly immunogenic antigen from SARS-CoV-2 by covalent coupling of the receptor binding domain of spike protein to a multimeric carrier. Preprint at bioRxiv. https://doi.org/10.1101/2021.04.25.441271.

Blanco-Melo, D., Nilsson-Payant, B.E., Liu, W.C., Uhl, S., Hoagland, D., Møller, R., Jordan, T.X., Oishi, K., Panis, M., Sachs, D., et al. (2020). Imbalanced host response to SARS-CoV-2 drives development of COVID-19. Cell *181*, 1036–1045.e9. https://doi.org/10.1016/j.cell.2020.04.026.

Bruchez, A., Sha, K., Johnson, J., Chen, L., Stefani, C., McConnell, H., Gaucherand, L., Prins, R., Matreyek, K.A., Hume, A.J., et al. (2020). MHC class II transactivator CIITA induces cell resistance to ebola virus and SARS-like coronaviruses. Science *370*, 241–247. https://doi.org/10.1126/science.abb3753.

Chen, J., Wang, R., Wang, M., and Wei, G.W. (2020a). Mutations strengthened SARS-CoV-2 infectivity. J. Mol. Biol. *432*, 5212–5226. https://doi.org/10.1016/j.jmb.2020.07.009.

Chen, W.H., Chag, S.M., Poongavanam, M.V., Biter, A.B., Ewere, E.A., Rezende, W., Seid, C.A., Hudspeth, E.M., Pollet, J., McAtee, C.P., et al. (2017). Optimization of the production process and characterization of the yeast-expressed SARS-CoV recombinant receptor-binding domain (RBD219-N1), a SARS vaccine candidate. J. Pharmacol. Sci. *106*, 1961–1970. https://doi.org/10.1016/j.xphs.2017.04.037.

Chen, W.H., Strych, U., Hotez, P.J., and Bottazzi, M.E. (2020b). The SARS-CoV-2 vaccine pipeline: an overview. Curr. Trop. Med. Rep. *7*, 61–64. https://doi.org/10.1007/s40475-020-00201-6.

Clover Biopharm (2020). Clover Initiates Development of Recombinant Subunit-Trimer Vaccine for Wuhan Coronavirus (2019-nCoV) (Clover Biopharm).

Cornelissen, L.A.H.M., de Vries, R.P., de Boer-Luijtze, E.A., Rigter, A., Rottier, P.J.M., and de Haan, C.A.M. (2010). A single immunization with soluble recombinant trimeric hemagglutinin protects chickens against highly pathogenic avian influenza virus H5N1. PLoS One *5*, e10645. https://doi.org/10.1371/journal.pone.0010645.

Crawford, K.H.D., Eguia, R., Dingens, A.S., Loes, A.N., Malone, K.D., Wolf, C.R., Chu, H.Y., Tortorici, M.A., Veesler, D., Murphy, M., et al. (2020). Protocol and reagents for pseudotyping lentiviral particles with SARS-CoV-2 spike protein for neutralization assays. Viruses *12*, 513. https://doi.org/10.3390/v12050513.

Custódio, T.F., Das, H., Sheward, D.J., Hanke, L., Pazicky, S., Pieprzyk, J., Sorgenfrei, M., Schroer, M.A., Gruzinov, A.Y., Jeffries, C.M., et al. (2020). Selection, biophysical and structural analysis of synthetic nanobodies that effectively neutralize SARS-CoV-2. Nat. Commun. *11*, 1–11. https://doi.org/10.1038/s41467-020-19204-y.

Fanslow, W.C., Clifford, K.N., Seaman, M., Alderson, M.R., Spriggs, M.K., Armitage, R.J., and Ramsdell, F. (1994). Recombinant CD40 ligand exerts potent biologic effects on T cells. J. Immunol. *152*, 4262–4269.

Gillies, S., and Stollar, V. (1980). Generation of defective interfering particles of vesicular stomatitis virus in Aedes albopictus cells. Virology *107*, 497–508. https://doi.org/10.1016/0042-6822(80)90316-5.

Goodwin, K., Viboud, C., and Simonsen, L. (2006). Antibody response to influenza vaccination in the elderly: a quantitative review. Vaccine *24*, 1159–1169. https://doi.org/10.1016/j.vaccine.2005.08.105.

Guo, L., Bi, W., Wang, X., Xu, W., Yan, R., Zhang, Y., Zhao, K., Li, Y., Zhang, M., Cai, X., et al. (2020). Engineered trimeric ACE2 binds viral spike protein and locks it in "Three-up" conformation to potently inhibit SARS-CoV-2 infection. Cell Res. *31*, 98–100. https://doi.org/10.1038/s41422-020-00438-w.

Harbury, P.B., Kim, P.S., and Alber, T. (1994). Crystal structure of an isoleucine-zipper trimer. Nature *371*, 80–83. https://doi.org/10.1038/371080a0.

He, Y., Zhou, Y., Liu, S., Kou, Z., Li, W., Farzan, M., and Jiang, S. (2004). Receptor-binding domain of SARS-CoV spike protein induces highly potent neutralizing antibodies: implication for developing subunit vaccine. Biochem. Biophys. Res. Commun. *324*, 773–781. https://doi.org/10.1016/j.bbrc.2004.09.106.

Herrera, N.G., Morano, N.C., Celikgil, A., Georgiev, G.I., Malonis, R.J., Lee, J.H., Tong, K., Vergnolle, O., Massimi, A.B., Yen, L.Y., et al. (2021). Characterization of the SARS-CoV-2 S protein: biophysical, biochemical, structural, and antigenic analysis. ACS Omega *6*, 85–102. https://doi.org/10.1021/acsomega.0c03512.

Hoffmann, M., Kleine-Weber, H., Schroeder, S., Krüger, N., Herrler, T., Erichsen, S., Schiergens, T.S., Herrler, G., Wu, N.H., Nitsche, A., et al. (2020). SARS-CoV-2 cell entry depends on ACE2 and TMPRSS2 and is blocked by a clinically proven protease inhibitor. Cell *181*, 271–280.e8. https://doi.org/10.1016/j.cell.2020.02.052.

Huang, Y., Yang, C., Xu, X.F., Xu, W., and Liu, S.W. (2020). Structural and functional properties of SARS-CoV-2 spike protein: potential antivirus drug development for COVID-19. Acta

Pharmacol. Sin. *41*, 1141–1149. https://doi.org/10.1038/s41401-020-0485-4.

Jackson, L.A., Anderson, E.J., Rouphael, N.G., Roberts, P.C., Makhene, M., Coler, R.N., McCullough, M.P., Chappell, J.D., Denison, M.R., Stevens, L.J., et al. (2020). An mRNA vaccine against SARS-CoV-2 — preliminary report. N. Engl. J. Med. *383*, 1920–1931. https://doi.org/10.1056/NEJMoa2027906.

Jiang, S., Bottazzi, M.E., Du, L., Lustigman, S., Tseng, C.T.K., Curti, E., Jones, K., Zhan, B., and Hotez, P.J. (2012). Roadmap to developing a recombinant coronavirus S protein receptor-binding domain vaccine for severe acute respiratory syndrome. Expert Rev. Vaccines *11*, 1405–1413. https://doi.org/10.1586/erv.12.126.

Kim, S., Liu, Y., Lei, Z., Dicker, J., Cao, Y., Zhang, X.F., and Im, W. (2021). Differential interactions between human ACE2 and spike RBD of SARS-CoV-2 variants of concern. J. Chem. Theory Comput. *17*, 7972–7979. https://doi.org/10.1021/acs.jctc.1c00965.

Kirchdoerfer, R.N., Cottrell, C.A., Wang, N., Pallesen, J., Yassine, H.M., Turner, H.L., Corbett, K.S., Graham, B.S., McLellan, J.S., and Ward, A.B. (2016). Pre-fusion structure of a human coronavirus spike protein. Nature *531*, 118–121. https://doi.org/10.1038/nature17200.

Lan, J., Ge, J., Yu, J., Shan, S., Zhou, H., Fan, S., Zhang, Q., Shi, X., Wang, Q., Zhang, L., and Wang, X. (2020). Structure of the SARS-CoV-2 spike receptor-binding domain bound to the ACE2 receptor. Nature *581*, 215–220. https://doi.org/10.1038/s41586-020-2180-5.

Li, Q., Wu, J., Nie, J., Zhang, L., Hao, H., Liu, S., Zhao, C., Zhang, Q., Liu, H., Nie, L., et al. (2020). The impact of mutations in SARS-CoV-2 spike on viral infectivity and antigenicity. Cell *182*, 1284–1294. https://doi.org/10.1016/j.cell.2020.07.012.

Liu, H., Zhang, Q., Wei, P., Chen, Z., Aviszus, K., Yang, J., Downing, W., Jiang, C., Liang, B., Reynoso, L., et al. (2021). The basis of a more contagious 501Y.V1 variant of SARS-CoV-2. Cell Res. *31*, 720–722. https://doi.org/10.1038/s41422-021-00496-8.

Loeffen, W.L.A., de Vries, R.P., Stockhofe, N., van Zoelen-Bos, D., Maas, R., Koch, G., Moormann, R.J., Rottier, P.J.M., and de Haan, C.A.M. (2011). Vaccination with a soluble recombinant hemagglutinin trimer protects pigs against a challenge with pandemic (H1N1) 2009 influenza virus. Vaccine *29*, 1545–1550. https://doi.org/10.1016/j.vaccine.2010.12.096.

Malladi, S.K., Patel, U.R., Singh, R., Pandey, S., Kumar, S., Gayathri, S., Kalita, P., Pramanick, I., Reddy, P., Girish, N., et al. (2021). A highly thermotolerant, trimeric SARS-CoV-2 receptor binding domain derivative elicits high titers of neutralizing antibodies. Preprint at bioRxiv. https://doi.org/10.1101/2021.01.13.426626.

Melchers, M., Matthews, K., de Vries, R.P., Eggink, D., van Montfort, T., Bontjer, I., van de Sandt, C., David, K., Berkhout, B., Moore, J.P., and Sanders, R.W. (2011). A stabilized HIV-1 envelope glycoprotein trimer fused to CD40 ligand targets and activates dendritic cells. Retrovirology *8*, 48. https://doi.org/10.1186/1742-4690-8-48.

Moderna. (2020). Moderna's COVID-19 Vaccine Candidate Meets its Primary Efficacy Endpoint in the First Interim Analysis of the Phase 3 COVE Study (Press Release).

Morris, A.E., Remmele, R.L., Klinke, R., Macduff, B.M., Fanslow, W.C., and Armitage, R.J. (1999). Incorporation of an isoleucine zipper motif enhances the biological activity of soluble CD40L (CD154). J. Biol. Chem. *274*, 418–423. https://doi.org/10.1074/jbc.274.1.418.

Morris, N.P., Peters, C., Montler, R., Hu, H.M., Curti, B.D., Urba, W.J., and Weinberg, A.D. (2007). Development and characterization of recombinant human Fc:OX40L fusion protein linked via a coiled-coil trimerization domain. Mol. Immunol. *44*, 3112–3121. https://doi.org/10.1016/j.molimm.2007.02.004.

Nguyen, H.L., Lan, P.D., Thai, N.Q., Nissley, D.A., O'Brien, E.P., and Li, M.S. (2020). Does SARS-CoV-2 bind to human ACE2 more strongly than does SARS-CoV? J. Phys. Chem. B *124*, 7336–7347. https://doi.org/10.1021/acs.jpcb.0c04511.

Ortega, J.T., Serrano, M.L., Pujol, F.H., and Rangel, H.R. (2020). Role of changes in SARS-CoV-2 spike protein in the interaction with the human ACE2 receptor: an in silico analysis. EXCLI J. *19*, 410–417. https://doi.org/10.17179/excli2020-1167.

Ramakrishnan, P., Wang, W., and Wallach, D. (2004). Receptor-specific signaling for both the alternative and the canonical NF-κB activation pathways by NF-κB-inducing kinase. Immunity *21*, 477–489. https://doi.org/10.1016/j.immuni.2004.08.009.

Rigter, A., Widjaja, I., Versantvoort, H., Coenjaerts, F.E.J., van Roosmalen, M., Leenhouts, K., Rottier, P.J.M., Haijema, B.J., and de Haan, C.A.M. (2013). A protective and safe intranasal RSV vaccine based on a recombinant prefusion-like form of the F protein bound to bacterium-like particles. PLoS One *8*, e71072. https://doi.org/10.1371/journal.pone.0071072.

Rose, A., Triano, C., Alatovic, J., and Maas, S. (2020). PFIZER AND BIONTECH conclude phase 3 study of covid-19 vaccine candidate, meeting all primary efficacy endpoints (Pfizer Inc).

Routhu, N.K., Cheedarla, N., Bollimpelli, V.S., Gangadhara, S., Edara, V.V., Lai, L., Sahoo, A., Shiferaw, A., Styles, T.M., Floyd, K., et al. (2021). SARS-CoV-2 RBD trimer protein adjuvanted with Alum-3M-052 protects from SARS-CoV-2 infection and immune pathology in the lung. Nat. Commun. *12*, 1–15. https://doi.org/10.1038/s41467-021-23942-y.

Rozanov, D.V., Savinov, A.Y., Golubkov, V.S., Rozanova, O.L., Postnova, T.I., Sergienko, E.A., Vasile, S., Aleshin, A.E., Rega, M.F., Pellecchia, M., and Strongin, A.Y. (2009). Engineering a leucine zipper-TRAIL homotrimer with improved cytotoxicity in tumor cells. Mol. Cancer Therapeut. *8*, 1515–1525. https://doi.org/10.1158/1535-7163.MCT-09-0202.

Schneider, C., Rasband, W., and Eliceiri, K. (2012). NIH image to ImageJ: 25 years of image analysis. Nat. Methods *9*, 671–675. https://doi.org/10.1038/nmeth.2089.

Seganti, L., Superti, F., Girmenia, C., Melucci, L., and Orsi, N. (1986). Study of receptors for vesicular stomatitis virus in vertebrate and invertebrate cells. Microbiologica *9*, 259–267.

Shang, J., Ye, G., Shi, K., Wan, Y., Luo, C., Aihara, H., Geng, Q., Auerbach, A., and Li, F. (2020). Structural basis of receptor recognition by SARS-CoV-2. Nature *581*, 221–224. https://doi.org/10.1038/s41586-020-2179-y.

Sliepen, K., Van Montfort, T., Melchers, M., Isik, G., and Sanders, R.W. (2015). Immunosilencing a highly immunogenic protein trimerization domain. J. Biol. Chem. *290*, 7436–7442. https://doi.org/10.1074/jbc.M114.620534.

Tai, W., He, L., Zhang, X., Pu, J., Voronin, D., Jiang, S., Zhou, Y., and Du, L. (2020). Characterization of the receptor-binding domain (RBD) of 2019 novel coronavirus: implication for development of RBD protein as a viral attachment inhibitor and vaccine. Cell. Mol. Immunol. *17*, 613–620. https://doi.org/10.1038/s41423-020-0400-4.

Tian, X., Li, C., Huang, A., Xia, S., Lu, S., Shi, Z., Lu, L., Jiang, S., Yang, Z., Wu, Y., and Ying, T. (2020). Potent binding of 2019 novel coronavirus spike protein by a SARS coronavirus-specific human monoclonal antibody. Emerg. Microb. Infect. *17*, 382–385. https://doi.org/10.1080/22221751.2020.1729069.

Vonderheide, R.H., Dutcher, J.P., Anderson, J.E., Eckhardt, S.G., Stephans, K.F., Razvillas, B., Garl, S., Butine, M.D., Perry, V.P., Armitage, R.J., et al. (2001). Phase I study of recombinant human CD40 ligand in cancer patients. J. Clin. Oncol. *19*, 3280–3287. https://doi.org/10.1200/JCO.2001.19.13.3280.

Walls, A.C., Park, Y.J., Tortorici, M.A., Wall, A., McGuire, A.T., and Veesler, D. (2020). Structure, function, and antigenicity of the SARS-CoV-2 spike glycoprotein. Cell *181*, 281–292. https://doi.org/10.1016/j.cell.2020.02.058.

Walls, A.C., Tortorici, M.A., Bosch, B.J., Frenz, B., Rottier, P.J.M., DiMaio, F., Rey, F.A., and Veesler, D. (2016). Cryo-electron microscopy structure of a coronavirus spike glycoprotein trimer. Nature *531*, 114–117. https://doi.org/10.1038/nature16988.

Walsh, E.E., Frenck, R.W., Falsey, A.R., Kitchin, N., Absalon, J., Gurtman, A., Lockhart, S., Neuzil, K., Mulligan, M.J., Bailey, R., et al. (2020). Safety and immunogenicity of two RNA-based covid-19 vaccine candidates. N. Engl. J. Med. *383*, 2439–2450. https://doi.org/10.1056/nejmoa2027906.

Wang, Q., Zhang, Y., Wu, L., Niu, S., Song, C., Zhang, Z., Lu, G., Qiao, C., Hu, Y., Yuen, K.Y., et al. (2020). Structural and functional basis of SARS-CoV-2 entry by using human ACE2. Cell *181*, 894–904.e9. https://doi.org/10.1016/j.cell.2020.03.045.

Wang, S., Dong, Z.Y., and Yan, Y.B. (2014). Formation of high-order oligomers by a hyperthemostable Fe-superoxide dismutase (tcSOD). PLoS One *9*, e109657. https://doi.org/10.1371/journal.pone.0109657.

Wrapp, D., Wang, N., Corbett, K.S., Goldsmith, J.A., Hsieh, C.L., Abiona, O., Graham, B.S., and McLellan, J.S. (2020). Cryo-EM structure of the 2019-nCoV spike in the prefusion conformation. Science *367*, 1260–1263. https://doi.org/10.1126/science.abb2507.

Xiao, T., Lu, J., Zhang, J., Johnson, R.I., McKay, L.G.A., Storm, N., Lavine, C.L., Peng, H., Cai, Y., Rits-Volloch, S., et al. (2021). A trimeric human angiotensin-converting enzyme 2 as an anti-SARS-CoV-2 agent. Nat. Struct. Mol. Biol. *28*, 202–209. https://doi.org/10.1038/s41594-020-00549-3.

Xiong, X., Qu, K., Ciazynska, K.A., Hosmillo, M., Carter, A.P., Ebrahimi, S., Ke, Z., Scheres, S.H.W., Bergamaschi, L., Grice, G.L., et al. (2020). A thermostable, closed SARS-CoV-2 spike protein trimer. Nat. Struct. Mol. Biol. *27*, 934–941. https://doi.org/10.1038/s41594-020-0478-5.

Yang, J., Wang, W., Chen, Z., Lu, S., Yang, F., Bi, Z., Bao, L., Mo, F., Li, X., Huang, Y., et al. (2020). A vaccine targeting the RBD of the S protein of SARS-CoV-2 induces protective immunity. Nature *568*, 572–577. https://doi.org/10.1038/s41586-020-2599-8.

Zhou, P., Yang, X.L., Wang, X.G., Hu, B., Zhang, L., Zhang, W., Si, H.R., Zhu, Y., Li, B., Huang, C.L., et al. (2020). A pneumonia outbreak associated with a new coronavirus of probable bat origin. Nature *579*, 270–273. https://doi.org/10.1038/s41586-020-2012-7.

Zhu, N., Zhang, D., Wang, W., Li, X., Yang, B., Song, J., Zhao, X., Huang, B., Shi, W., Lu, R., et al. (2020). A novel coronavirus from patients with pneumonia in China, 2019. N. Engl. J. Med. *382*, 727–733. https://doi.org/10.1056/nejmoa2001017.

STAR★METHODS

KEY RESOURCES TABLE

REAGENT or RESOURCE	SOURCE	IDENTIFIER
Antibodies		
ACE2 Rabbit Ab	Cell signaling	#4355S; RRID:AB_2797606
ACE2 Rabbit Ab	Abcam	#Ab15348; RRID:
Monoclonal Anti-FLAG M2 antibody produced in mouse	Sigma Aldrich	#F1804; RRID:
Purified anti-DYKDDDDK tag antibody	BioLegend	637319
Anti-DYKDDDDK tag (L5) affinity gel antibody FLAG beads	BioLegend	651501
Anti-FLAG M2 affinity Gel	Millipore Sigma	#A2220
Monoclonal Anti-HIS tag antibody produced in mouse	Sigma Aldrich	#SAB1305538; RRID:AB_2687993
Anti-Mouse IgG HRP conjugate	Cell signaling	Cat#7076s; RRID:AB_330924
Anti-Rabbit IgG HRP conjugate	Cell signaling	Cat#7074s; RRID:AB_2099233
Bacterial and virus strains		
SARS CoV-2 isolate USA-WA1/2020	BEI Resources	NR-52281
Chemicals, peptides, and recombinant proteins		
Recombinant SARS COV-2 spike protein (RBD HIS tag)	Sino biological Inc	#40592-V088 LC1MC 1106
Biotinylated Recombinant human ACE2	Abclonal	#RP02269
Ni-NTA Agarose	QIAGEN	#30210
Polybrene	Millipore sigma	#TR-1003-G
Amicon ultra-15 centrifugal filters	Millipore sigma	#UFC9050
Critical commercial assays		
Dual-Luciferase reporter assay system	Promega	#E1960
Experimental models: Cell lines		
VERO-E6 cells	ATCC	CRL-1586
HEK293T cells	ATCC	CRL-3216
HEK293T-ACE2 cells	Crawford et al., 2020	Gift (Dr. Jesse D Bloom)
Recombinant DNA		
SARS-CoV2 Spike-ALAYT, pHAGE-CMV-Luc2-IRES-Zsgreen, HDM-HgPM2, HDM-tat1b, PRC-CMV-Rev1b plasmids	Gift (Dr. Jesse D Bloom)	Crawford et al. (2020)
SARS-CoV-2 (2019-nCoV) Spike (RBD) ORF mammalian expression plasmid, N-His tag	Sino biological Inc	#VG40592-NH
Software and algorithms		
Prism software V9.1.0	GraphPad	GraphPad
ImageJ	Schneider et al., 2012	https://imagej.nih.gov/ij/
Other		
Sensor Chip SA	Cytiva	Cat#29104992
15Q column with SOURCE 15Q beads	GE Healthcare	Cat# 17-0947-20

RESOURCE AVAILABILITY

Lead contact

Information and requests for resources and reagents should be directed to and will fulfilled by Dr. Parameswaran Ramakrishnan (pxr150@case.edu).

Materials availability

Plasmids generated specifically for this study are available upon request.

Data and code avilibility

- Reagent identifiers are listed in the key resources table.
- This paper does not report original code.
- Any additional information required to reanalyze the data reported in this paper is available from the lead contact upon request [Lead contact: Dr. Parameswaran Ramakrishnan (pxr150@case.edu).

EXPERIMENTAL MODEL AND SUBJECT DETAILS

Cells

Vero-E6, HEK293T, HEK293T cells stably expressing ACE2 protein (HEK293T-ACE2) were grown in complete DMEM media supplemented with 2 mM L-glutamine, 100 U/mL penicillin/streptomycin, and 10% heat inactivated FBS (Sigma Aldrich).

Virus

SARS CoV-2 isolate USA-WA1/2020 was obtained from BEI Resources, NIAID, NIH (full designation: SARS-Related Coronavirus 2, Isolate USA-WA1/2020, NR-52281, deposited by the Centers for Disease Control and Prevention).

METHOD DETAILS

Molecular modeling

The leucine (GCN4) zipper was used as a template (PDB 4dme) to model the structure of modified leucine zipper (**MKQIEDKIEEILSKIYHIENEIARIKKLIGERLDP**). This modified sequence is known to form coiled-coil trimers (Fanslow et al., 1994)The leucine zipper was fused to three spike RBD (319–541) via a flexible linker with sequence HHHHHHHHHHGGGGS. ACE2 are docked to RBDs with template of ACE2:RBD binding structure (PDB, 6m17). The linker region between RBD and leucine zipper is long and flexible. We explored the binding modes of leucine zipper RBD timer with one or multiple ACE2 dimer.

Recombinant protein expression and purification

The cDNA for RBD was purchased from Sino Biological (Cat# VG40592-NH) and cloned in fusion with a leader sequence, a modified leucine zipper that allows trimer formation (Fanslow et al., 1994), and FLAG or HIS tag into the mammalian expression vector pcDNA3, as previously described (Ramakrishnan et al., 2004). The mammalian expression vector expressing secreted monomeric HIS tagged RBD (pCAGGS-HIS RBD) was kindly provided by Dr. Florian Krammer, Icahn School of Medicine at Mount Sinai, New York.

Recombinant tRBD and mRBD proteins were produced via transient transfection of HEK293T cells using calcium phosphate precipitation. Cells were washed twice with PBS after 6 hours and incubated in fresh 2% FBS DMEM. Culture medium containing tRBD and mRBD was collected after 72 hours, centrifuged, and passed through a 0.45 μm syringe filter. tRBD and mRBD conditioned media were stored at −80°C until use. Expression of tRBD and mRBD was confirmed by Western blotting.

To purify tRBD, fresh cleared conditioned media containing tRBD was loaded onto a column packed with washed Ni-NTA beads (5 mL beads/500 mL media; Cat#30210) equilibrated with equilibration buffer (20 mM sodium phosphate pH 7.4; 0.5 M NaCl). Beads were sequentially washed with washing buffer (20 mM sodium phosphate pH 7.4; 0.5 M NaCl) containing 10, 20 and 30 mM imidazole to remove nonspecific protein binding. Bound proteins were eluted using elution buffer (20 mM sodium phosphate pH 7.4; 0.5 M NaCl) containing 250 mM imidazole. The eluted fraction was dialyzed against Tris-NaCl buffer (25 mM Tris pH 7.4; and 25 mM NaCl) to remove imidazole and concentrated using spin columns (MWCO 50 kDa)

prior to ion-exchange chromatography. The concentrated protein samples were loaded on a MonoQ column equilibrated with Tris-NaCl buffer (25 mM Tris pH 7.4; and 25 mM NaCl) using an AKTA FPLC system. The eluted fractions containing tRBD were dialyzed against PBS (pH 7.4) and concentrated in spin columns (MWCO 50 kDa). Purified tRBD was stored at −80°C until further use.

Quantification of secreted tRBD and mRBD in culture media

Concentrations of tRBD and mRBD in the culture supernatants were estimated by western blot and densitometry analysis. Densitometry analysis of bands was done using ImageJ software (NIH). A standard curve was generated using incremental concentrations of recombinant RBD (Sino Biological, Cat.# 40592-V08B) and a regression equation was obtained. Concentrations of tRBD or mRBD were then calculated per the regression equation.

Chemical crosslinking of tRBD

Chemical crosslinking of tRBD was carried out as previously described (Wang et al., 2014). Briefly, 2.5% glutaraldehyde was added to the purified tRBD (20 μg/mL) in PBS and incubated at 25°C or 80°C for 5 min. The reaction was stopped by adding 1M Tris-HCl and proteins were analyzed by Western blot.

Immunoprecipitation and western blotting

HEK 293T-ACE2 cells were cultured to 90% confluency and treated with HIS-tagged or FLAG-tagged tRBD or mRBD media for 30 minutes. Cells were lysed in lysis buffer (1.0% Triton-X100, 20 mM HEPES [pH 7.6], 0.1% SDS, 0.5% Sodium deoxycholate, 150 mM NaCl, 1 mM EDTA and complete protease inhibitor cocktail) for 15 minutes on ice. Immunoprecipitation was carried out at 4°C for 2 hours using anti-FLAG M2 agarose beads (Sigma; Cat# A2220) or Ni-NTA agarose beads (Qiagen; Cat#30210). For Western blot analysis, cell lysates as well as immunoprecipitates were resolved through 12% SDS-PAGE gels. Proteins from gels were transferred onto nitrocellulose membranes, probed using relevant antibodies, and visualized via enhanced chemiluminescence reagent.

Surface plasmon resonance

SPR studies were performed using a BIAcore T200 device (Cytiva) at 25°C. Chamber temperature was set at 10°C to store protein samples. The binding assays were conducted in PBSP + buffer, containing 20 mM phosphate (pH 7.4), 137 mM NaCl and 2.7mM KCl, plus 0.05% surfactant Tween-20. Next, biotin-ACE2 was captured on an S-series SA sensor chip (BIAcore) at a density ranging from 500-1500RU on different flow cells. Three-fold series of tRBD ranging from 0.237 nM to 19.19nM (12.35 nM to 1000 nM for mRBD) were then injected at a rate of 30 μL/min over surfaces using the single-cycle kinetics method. The dissociation time for mRDB was 600s and that of tRBD was extended to 3000s due to its slow off-rate. Each data point was repeated at least three times and double referencing was applied to all detected traces using BIAevaluation software (version 3.1). The binding data were globally fitted to a 1:1 Langmuir binding model. Sensorgrams were redrawn using Origin 2017 software.

Luciferase assay

Pseudotyped SARS-CoV-2 spike protein and neutralization assays were performed as previously described (Crawford et al., 2020). Briefly, HEK293T cells were co-transfected with SARS-CoV-2 spike-ALAYT, pHAGE-CMV-Luc2-IRES-Zsgreen, HDM-HgPM2, HDM-tat1b, PRC-CMV-Rev1b plasmids (generously gifted from Dr. Jesse D Bloom). Culture supernatant was collected after 48 hours and passed through a 45 μM filter and stored at −80°C until use.

For neutralization assay, HEK293T-ACE2 cells were plated in a 96 well plate (1.25×10^4 cells/well) overnight. Cells were incubated with undiluted spike pseudotyped virus or 1:50 diluted VSVG pseudotyped virus along with indicated dilutions of tRBD and mRBD (final volume 200 μL/well) for 48 hours. 5 μg/mL polybrene was used to facilitate lentiviral infections. Luminescence was measured using luciferase assay system following manufacturer's instructions (Promega, Cat# E1960) on a Spectramax 3000 plate reader and results were plotted as relative light units (RLU).

SARS-CoV-2 plaque reduction assay

SARS-CoV-2 isolate USA-WA1/2020 was propagated and stocks were maintained as previously described (Bruchez et al., 2020). Twenty-four hours prior to infection 1×10^5 Vero E6 cells per well were plated in

24-well plates such that cells would be at least 90% confluent at the time of infection. The following day, two-fold serial dilutions of mRBD, tRBD, and mock (Mk) conditioned media were prepared in virus media to the concentrations indicated in the figures. Confluent cell monolayers of Vero E6 cells were incubated with 250 μL of diluted mRBD, tRBD, or Mk media for 30 minutes at 37°C, with gentle rocking after 15 minutes. After incubation with conditioned media, each well received 50μL of SARS-CoV-2 diluted in virus media at a dilution of 10^{-4} and plates were incubated for 1 hour at 37°C, using 24-well plates, with gentle rocking every 15 minutes. Following incubation for one hour, each well received 500 μL of overlay medium containing DMEM with 0.05% agarose and 2% FBS followed by 72 hours incubation at 37°C. After cells were fixed using a 4% formaldehyde solution in PBS for 30 minutes and stained with crystal violet for 5 minutes. Viral titers of SARS-CoV-2 were measured by counting the number of plaque-forming units (PFU) per well and then considering dilutions to back-calculate plaque-forming units per milliliter (PFU/mL). To combine multiple individual experiments for IC50 calculations, values were normalized to Mk media for each dilution and IC50 values were calculated using the concentration of inhibitor vs normalized response with a variable slope in Prism software (V9.1.0, GraphPad) and are presented with 95% confidence interval.

QUANTIFICATION AND STATISTICAL ANALYSIS

Statistical differences in gene expression were analyzed with a two-tailed Student's unpaired *t* test with Prism software (GraphPad). Data are presented as means ± SE of mean (SEM), unless otherwise indicated. ***$p < 0.001$, **$p < 0.01$, *$p < 0.05$. In statistical significance of true virus infection, error bars represent 95% confidence interval and significance was determined by ANOVA with Dunnett's multiple comparison tests. *$p < 0.05$; **$p < 0.01$; ***$p < 0.001$, ****$p < 0.0001$.